

# Understanding Cognitive States from Head & Hand Motion Data

Kaiang Wen\*

Mark Roman Miller†

Department of Computer Science  
Illinois Institute of Technology

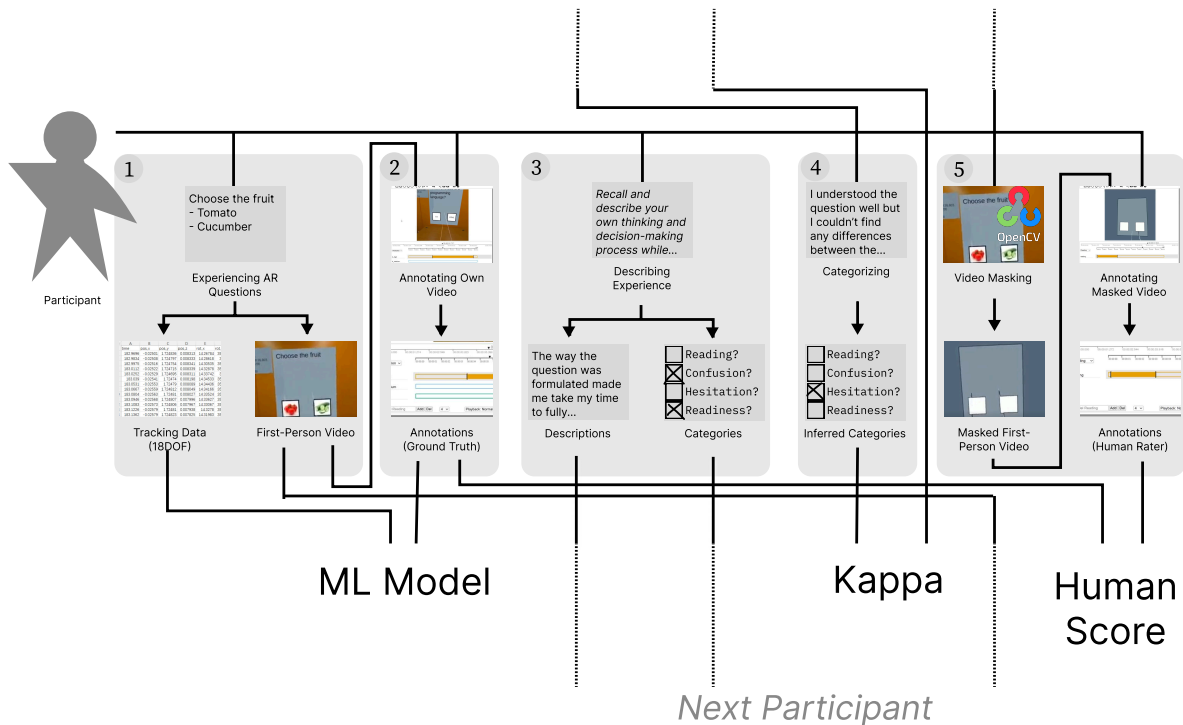


Figure 1: Overview of our study design. The pipeline illustrates the full workflow from data collection in VR, through self-annotation and human baseline evaluation, to modeling and analysis of cognitive states.

## ABSTRACT

As virtual reality (VR) and augmented reality (AR) continue to gain popularity, head and hand motion data captured by consumer VR systems have become ubiquitous. Prior work shows such telemetry can be highly identifying and reflect broad user traits, often aligning with intuitive “folk theories” of body language. However, it remains unclear to what extent motion kinematics encode more nuanced cognitive states, such as confusion, hesitation, and readiness, which lack clear correlates with motion. To investigate this, we introduce a novel dataset of head and hand motion with frame-level annotations of these states collected during structured decision-making tasks. Our findings suggest that deep temporal models can infer subtle cognitive states from motion alone, achieving comparable performance with human observers. This work demonstrates that standard VR telemetry contains strong patterns related to users’ internal cognitive processes, which opens the door for a new gener-

ation of adaptive virtual environments. To enhance reproducibility and support future work, we will make our dataset and modeling framework publicly available.

**Index Terms:** Virtual reality, kinematic analysis, cognitive state inference, machine learning.

## 1 INTRODUCTION

Virtual Reality (VR) is rapidly evolving from a specialized tool for simulation and entertainment into a mainstream computing platform for work, education, and social interaction. As users spend more time in these immersive environments, the quality of human-computer interaction becomes paramount. The next generation of VR systems must move beyond explicit, command-based interfaces and develop the capacity for implicit, nuanced understanding. This requires an ability to perceive and adapt to a user’s cognitive state in real-time, creating experiences that are more intuitive, supportive, and effective. The key to unlocking this capability lies in decoding the rich, continuous, and often subconscious stream of motion data generated by every user.

A growing body of research shows that motion carries rich signatures of internal states. It is intuitive that movement can reveal broad traits: slow or reduced motion has been linked to depression [35, 6], while posture and gesture can signal archetypal emotions

\*e-mail: kwen2@hawk.illinois.edu

†e-mail: mmiller30@illinois.edu

[24]. These findings echo common “folk theories” of body language. Yet the ceiling for what motion can reveal is likely much higher than intuition suggests. For example, it is unsurprising that a face in a photograph can identify a person, but less obvious that the unique current drawn by household appliances can reveal which devices are active from a single outlet [7]. In VR, head and hand trajectories can be so distinctive that they act as biometric fingerprints [21], identifying users among tens of thousands [22]. If motion can reveal who a user is, could it also reveal what they are thinking moment to moment?

The link between motion kinematics and the subtle, moment-to-moment cognitive states that lack clear physical correlates remains unexplored. This leads to our research questions: *Is it possible to use solely head and hand motion to infer human’s nuanced cognitive states, such as confusion, hesitation, and readiness? And how well can machine learning models perform on this task compared to human observers?*

Our work addresses this counterintuitive frontier by focusing on fine-grained cognitive states during user’s decision-making: confusion, hesitation, and readiness, that lack clear, observable correlates in body language. While prior research has shown that motion can capture mood or general affect [24], and physiological sensing can capture workload or stress [33, 18], no study has systematically tested whether head and hand motion captured by consumer VR system alone is indicative of these subtle, nuanced cognitive processes. To investigate this problem, we introduce a new dataset of head and hand motion paired with frame-level self-annotations of reading, confusion, hesitation, and readiness, collected during structured decision-making tasks. We then evaluate whether machine learning models can reveal nuanced cognitive states from motion alone and compare their performance to that of human observers. This study provides the first systematic evidence that standard VR motion telemetry is identifying for nuanced cognitive states, opening the door to adaptive VR systems that anticipate and respond to users’ unspoken needs.

Our contributions can be summarized as follows:

- We introduce a novel dataset of VR head and hand motion, synchronized with frame-level annotations of reading, confusion, hesitation, and readiness.
- We provide the first systematic evidence that subtle cognitive states can be inferred from standard VR telemetry.
- We conducted extensive experiments to evaluate classical, convolutional, and recurrent models against a human baseline, identifying strengths and limits of each.
- We discuss the challenges of subject-independent generalization and highlight both opportunities for adaptive VR and the privacy risks.

## 2 RELATED WORK

Our research is situated at the intersection of two primary domains: the analysis of human motion from time-series data and the prediction of internal human states, such as emotions and cognitive processes, from behavioral signals. The literature in these areas has evolved from traditional statistical and machine learning models that rely on handcrafted features to end-to-end deep learning architectures that learn representations directly from data.

### 2.1 Inferring Internal States

**Motion as a Rich but Sensitive Signal.** The motion data from consumer VR systems is a rich source of information. This data is more than just a record of user actions. Prior studies show that head and hand motion can reveal broad user traits. The data can even act as a unique biomechanical identifier for a person. Thus, motion is a powerful yet sensitive signal that introduces privacy risks.

Our work uses this rich signal to decode the moment-to-moment changes in a user’s internal state.

**Contrast with Physiological Sensing.** Other research uses physiological sensors to understand users. These studies often use signals like EEG to recognize cognitive states or emotions. Classifiers like Support Vector Machines (SVMs) and Random Forests have been used on EEG data to predict cognitive states [3, 19]. These methods can be effective, but they require extra hardware that is not standard in consumer VR. Our work uses only the head and hand motion that standard headsets already track.

**Evidence of Specific State Markers.** Prior work has found links between motion and specific internal states. For example, researchers have used body movements to recognize emotions [11]. Other work in VR has used eye and hand data to predict a user’s attention state, where gradient boosting performed best among traditional models [4]. For states defined by their timing, like hesitation, specific methods are needed. Dynamic Time Warping (DTW) is an algorithm that is very good at handling variations in the speed of human movement [23, 15]. This makes it theoretically well-suited for temporal states like hesitation. These studies prove that specific states have motion markers.

**Decision-Making Context.** Our study investigates cognitive states within a structured decision-making task. The rational planning model describes five steps in a decision-making process: defining the problem or goal, identifying possible options, evaluating the options, making a choice, and monitoring the outcome [30], and has served as a reference for studying adaptive human choice [25] and provide the foundation for influential HCI theories such as information searching [26]. Regarding the three cognitive states our paper focuses on, confusion often arises when users try to define or understand the goal. Hesitation and readiness are more likely during evaluation and action, when users commit to a choice. In our VR tasks, participants could face ambiguous, confusing questions and mismatched options. This design is intentional to trigger this decision-making process, inducing confusion, hesitation, and readiness during the experiment.

## 2.2 Motion Analysis Methods

**Classical Models.** Classical machine learning models represent a foundational approach to motion analysis. This approach involves two main steps. First, researchers manually design and extract a set of features from the raw motion data. This turns a motion sequence into a fixed-size vector. Second, a standard classifier is trained on these features.

Feature-based classifiers such as Support Vector Machines (SVMs), Random Forests, and Gradient Boosting are widely used in Human Activity Recognition (HAR) and emotion recognition [29, 27]. Their performance depends completely on the quality of the handcrafted features. For subtle cognitive states, it is difficult to design features that capture complex motion patterns.

Similarity-based classifiers avoid manual feature design by comparing a new sequence to stored examples. Dynamic Time Warping (DTW) is the most common method [9, 31]. It is very effective at comparing human movements that may vary in speed, which makes it useful for posture recognition. However, it can be computationally expensive and hard to interpret.

**Deep Temporal Models.** Deep learning models instead learn feature representations directly from raw data, an approach called end-to-end learning. This is especially useful for complex time-series data such as motion.

Recurrent Neural Networks (RNNs) such as Long Short-Term Memory (LSTM) networks [8] are strong baselines for sequential data tasks [38]. They capture temporal dependencies using memory of prior time steps and have been applied in HAR and intention prediction.

Convolutional Neural Networks (CNNs) are also effective for



Figure 2: The experimental setup. (Left) The physical lab space where participants stood on the marked footprints. (Right) A screenshot of the in-VR view, showing an example question from the decision-making task.

time-series analysis. One-dimensional CNNs use filters to detect local patterns (“motifs”) in motion data [12]. They are computationally efficient and widely applied in HAR and emotion recognition [40].

Hybrid models combine CNNs and RNNs, where CNNs extract local patterns and RNNs model temporal relationships. These hybrids achieve strong results in HAR and affective computing [39].

Transformers [34] are the current state-of-the-art in sequence modeling. Their self-attention mechanism can capture long-range dependencies more effectively than RNNs. In motion analysis, spatio-temporal Transformers have been proposed to model posture and temporal dynamics jointly [1, 10, 20, 13, 37, 32]. They are also more interpretable, as attention weights can be visualized to reveal what the model focuses on during classification, a property widely demonstrated in machine learning domains including computer vision [36, 16] and natural language processing [17, 28].

### 3 METHOD

This section details participants, apparatus, task and procedure, signals and logging, annotation and time synchronization, dataset construction, features, models, training, and evaluation (including a human baseline).

#### 3.1 Participants and Ethics

We recruited 26 participants mainly from our university to take part in the experiment, and data collected from 2 of them were discarded due to data quality and completeness. The remaining 24 participants is consisting of 10 females, 11 males and 1 non-binary. They were university students or graduated students, aged 20-28 ( $M=23.8$ ,  $SD=2.81$ ). Among them, 3 individuals (12.5%) use VR devices more than once a week, 15 individuals (62.5%) have experienced VR devices before but are not frequent users, while 6 individuals (25.0%) have no prior experiences with VR devices.

All participants read and signed an IRB-approved consent form. A within-subject design was used, and all participants underwent the same experimental conditions.

#### 3.2 Apparatus

Experiments ran on a Meta Quest 3S HMD with two handheld controllers. The VR application was developed in Unity 2022.3.52f1. Participants stood in a fixed spot marked with stickers on the ground, wearing the HMD and holding both controllers with both hands. The VR question board was positioned directly in front of the participant; the experimenter remained at a fixed location, sitting at the left side of the participant. The experimental space setup is shown in Fig. 2.

#### 3.3 Task and Procedure

**VR session.** Each participant completed 30 randomized multiple-choice trials in VR. On each trial, a question with two candidate answers was presented on a virtual board. Participants read the question, considered the options, and selected the answer they believed correct. A short practice trial was provided before the main session.

After completing the VR task, participants engaged in two annotation phases:

**Self-annotation.** Participants reviewed their own session recordings, which had been segmented into 30 clips. For each clip, they marked the presence and intensity of Reading (binary) as an action, and three cognitive states: Confusion (low/medium/high), Hesitation (low/medium/high), and Readiness (low/medium/high), on the timeline. This procedure generated the ground-truth labels used in modeling.

**Human baseline.** To evaluate human’s ability in predicting cognitive states from motion, each participant also annotated a small set of masked video clips from the lexicographically preceding participant. These masked clips were generated by hiding the question text and answer options while preserving head and hand motion trajectories. With this design, human predictors predict the cognitive states from the lexicographically preceding participant with motion as the only given information. We then evaluate human’s performance by comparing human predictions with the lexicographically preceding participant’s self annotation, as a human baseline to compare with model’s performance on this task. Note that masked clips share the same start/end timestamps as the original trials; the opening segment typically corresponds to Reading, giving human raters a structural prior that can disproportionately benefit the Reading class. We report this caveat alongside results and include per-class analysis.

**Text-based description and rating.** To evaluate whether participants reach a consensus when annotating, e.g. what kinds of thinking process should be labeled as confusion/hesitation/readiness, we conduct a text-based describing and rating. Each participant, first acting as a descriptor, wrote plain-language accounts of their decision-making process for two randomly sampled questions (see supplementary material for full instructions). These written descriptions were then shown to other participants, who acted as raters. Raters judged whether the text reflected Confusion, Hesitation, or Readiness, evaluating each state independently (see supplementary material for rater instructions).

Together, these procedures produced a dataset containing ground-truth self-annotations and independent human judgments for comparison against model predictions.

#### 3.4 Signals and Logging

We recorded three tracker streams at 72 Hz: *head* (HMD), *left hand*, and *right hand*. Each CSV log contains columns *time*, *pos\_x*, *pos\_y*, *pos\_z*, *rot\_x*, *rot\_y*, *rot\_z*, where *time* is seconds on the Unity timeline shared across trackers. Positions are expressed in meters, and rotations are Euler angles in degrees. Unity’s default coordinate system was used without re-centering or smoothing.

The custom Unity application additionally logged Unity-based and local timestamps, as well as trial durations. A continuous VR camera recording of the session was also captured for annotation. This recording was later segmented into 30 trial-specific clips using the Unity timestamps, allowing participants to perform self-annotation with improved clarity and reduced cognitive load.

#### 3.5 Annotations and Ground Truth

For each trial clip, participants provided *self-annotations* of four cognitive states as temporal segments on the clip timeline: **Reading** (binary), **Confusion** (low/medium/high), **Hesitation**



Figure 3: The VIA annotation interface. (Left) Example of self-annotation, where participants reviewed their own VR session recordings. (Right) Example of human baseline evaluation, where participants inferred states from a previous participant's masked videos, with task text and options hidden but motion preserved. In this example, the predictor failed to detect the rater's hesitation in the trial.

(low/medium/high), and **Readiness** (low/medium/high). Overlaps across different states were permitted (e.g., Reading overlapping with Confusion). The annotation is done on VGG Image Annotator (VIA) [5], as shown in Fig. 3.

The four states were defined as follows:

- **Reading:** The initial period during which the participant reads the question and the two response options.
- **Confusion:** A state of uncertainty arising when task criteria are ambiguous or unclear (e.g., when the question is not well understood).
- **Hesitation:** A state in which the participant understands the task but delays the decision, often comparing between two options.
- **Readiness:** A state of clarity in which the participant fully understands the task and has committed to an option, but is waiting for the appropriate cue to act (e.g., waiting for the background color to change).

Within the same *single state*, if multiple intensity levels overlapped (e.g., Confusion\_high overlapping with Confusion\_med), we applied a simple correction by splitting the overlap at the midpoint, to ensure data quality. This was the only data cleaning step performed on the annotations.

If a clip contained no marks for Hesitation, Confusion, or Readiness, the corresponding state was treated as absent (all-zero) for that clip.

### 3.6 Human baseline

As shown in Fig. 3, to evaluate human ability to infer cognitive states from motion alone, each participant is instructed to annotate a subset of trial clips from the previous participant. All questions and options in the video clips were masked to obscure the context while preserving motion trajectories. Each annotator labeled between 6 and 10 clips. To ensure fairness, human performance was first averaged within each annotator and then across all annotators with equal subject weight. The first participant had no predecessor and was therefore excluded from baseline aggregation.

### 3.7 Dataset Construction

We enforced strict integrity requirements to ensure consistency across sessions. Each session was required to contain exactly 30 trials; sessions with missing trials were discarded. All tracker files had to be present with standardized filenames, and each session was paired with a single VR recording, a self-annotation file, and a prediction-last file, except for the first participant.

Tracker signals were preprocessed as follows. Euler angles were first unwrapped per axis to remove  $360^\circ$  discontinuities. All three tracker streams (head, left hand, right hand) were then resampled to a uniform 72 Hz grid using linear interpolation. Short gaps of at most two frames ( $\leq 27.8$  ms) were forward-filled, while longer gaps were dropped to preserve signal quality.

Annotations were rasterized onto the 72 Hz timeline to obtain framewise labels. For binary presence, each state  $c \in \{\text{Reading, Hesitation, Confusion, Readiness}\}$  was encoded as  $y_c(t) \in \{0, 1\}$ . For ordinal intensity,  $\{\text{low, medium, high}\}$  were mapped to  $\{1, 2, 3\}$  with 0 denoting absence, yielding  $y_c^{\text{lev}}(t) \in \{0, 1, 2, 3\}$  for Hesitation, Confusion, and Readiness (Reading remained binary).

To prepare data for modeling, we applied a sliding-window procedure. A causal window of width  $W = 2.0$  s ( $T = 2.0 \times 72$  frames) was advanced with a stride of  $s = 0.5$  s across the continuous session, producing training sequences  $X \in \mathbb{R}^{T \times F}$ .

### 3.8 Feature Extraction

We adopted the featurization strategy introduced by Nair et al. [22], which demonstrated state-of-the-art performance for user identification from VR motion data. Specifically, orientation was represented using four quaternion components  $(q_i, q_j, q_k, q_l)$  instead of Euler angles, as quaternions avoid singularities and provide more stable orientation encoding.

For each tracker stream (*head, left hand, right hand*), we computed per-axis statistics over short temporal windows. Each window was summarized using five statistical aggregators: minimum, maximum, mean, median, and standard deviation. These were applied to the position coordinates  $(pos_x, pos_y, pos_z)$  and quaternion orientation components  $(q_i, q_j, q_k, q_l)$ , yielding a compact feature representation.

The resulting feature vector is 105-dimensional, constructed as:

$$\begin{aligned} & \{pos_x, pos_y, pos_z, q_i, q_j, q_k, q_l\} \\ & \quad \times \\ & \{\min, \max, \text{mean}, \text{median}, \text{std}\} \\ & \quad \times \\ & \{\text{head, left hand, right hand}\}. \end{aligned}$$

All channels are normalized using z-score.

### 3.9 Model Selection

We evaluated both classical machine learning models and deep sequence models:

1. **Support Vector Machine (SVM)** as a strong classical baseline for binary classification.
2. **Random Forest (RF)** as a non-parametric ensemble method capable of handling nonlinear decision boundaries.
3. **LightGBM** as a gradient boosting approach optimized for efficiency and class imbalance.
4. **Long Short-Term Memory (LSTM)** networks to capture temporal dependencies in sequential motion data.
5. **ResNet-1D** to model local temporal patterns with residual connections for deeper architectures.

### 3.10 Training Setup

For each participant, data were split by time: the first 70% of each session was used for training and the remaining 30% for testing. Inputs were segmented into 2-second windows with a stride of 0.5 s at 72 Hz. Features were normalized using z-score, and data augmentation was applied during training (Gaussian jitter,  $\sigma = 0.05$ ; amplitude scaling, uniform [0.8, 1.2]).

Models were trained for 100 epochs using the Adam optimizer [14] (learning rate  $1 \times 10^{-4}$ , cosine decay to  $5 \times 10^{-6}$  after a 5-epoch warm-up, weight decay = 0.001). The batch size was 32, gradient clipping was set to 1.0, and dropout was 0.3. All runs used a fixed random seed 42.

The loss function we use was a weighted cross-entropy [2], with task-specific class weights estimated from the training distribution. These hyperparameters were shared across different models to achieve a fair comparison.

### 3.11 Evaluation Protocol

**Framework evaluation.** Model outputs are compared against frame-level ground truth labels for Reading, Confusion, Hesitation, and Readiness. For each state, we compute standard classification metrics: accuracy, precision, recall, and F1 at the frame level. Metrics are aggregated per subject and then averaged across subjects.

**Event-based IoU.** As illustrated in Fig. 4, large portions of the dataset contain no active labels (Confusion, Hesitation, and Readiness all absent). Therefore, we report event-based Intersection-over-Union (IoU) to evaluate human and model’s performance in detecting cognitive state’s existence. Event-based IoU is computed only over time intervals explicitly annotated by participants as containing at least one cognitive state. This metric evaluates whether models and human raters correctly predict *when* a state occurs.

**Human baseline.** For comparison, we evaluate human raters on the masked subset of clips. Metrics are first averaged within each participant and then across participants, giving equal weight for fairness. Reported values summarize overall human performance against self-annotated ground truth. Note that masked videos share the same start and end timestamps as the original sliced videos, retaining trial boundaries; consequently, video onsets typically align with Reading. This structural prior can inflate human accuracy on Reading relative to the three cognitive states—Confusion, Hesitation, and Readiness.

### 3.12 Implementation and Reproducibility

Experiments were conducted on Ubuntu 24.04.3LTS with Python 3.8.20 and PyTorch 2.4.1. Training and evaluation ran on a Lenovo Legion laptop with an RTX 3080 16 GB GPU; video slicing and annotation were performed on a Lenovo Yoga laptop with Intel i7-13700H CPU. The collected dataset, Unity application, and the full modeling code will be released publicly upon acceptance.

## 4 RESULTS

### 4.1 Dataset distributions.

To better understand the distribution of annotated states, we visualize the dataset in terms of both prevalence and intensity Fig. 4. The top panel shows the fraction of time each state was annotated as present across subjects. Reading and hesitation were the most frequently observed, while confusion and readiness appeared less often. This indicates that participants were consistently engaged in reading and decision evaluation, but displayed confusion and readiness more sparsely.

The bottom panel illustrates the intensity distributions for confusion, hesitation, and readiness. Among marked annotations (low/med/high), confusion was typically marked at high levels, with relatively few medium or high annotations. Hesitation showed

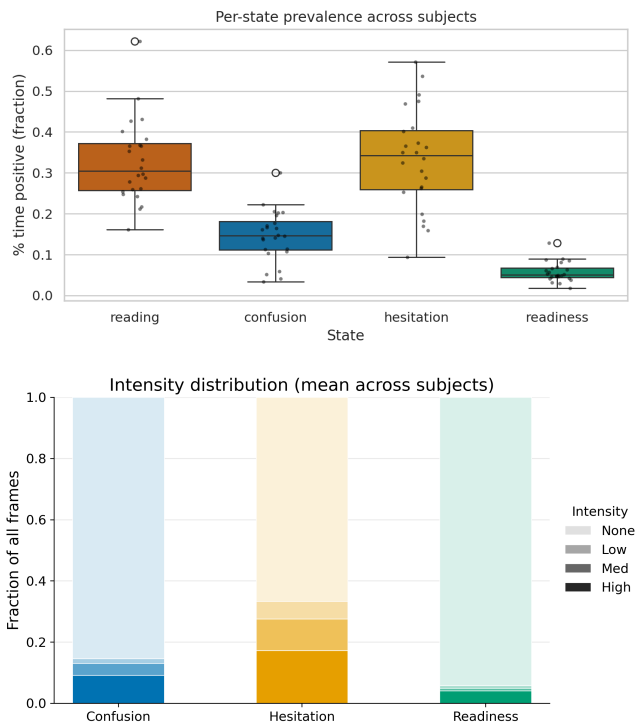


Figure 4: Distribution of annotated cognitive states across the dataset. (Top) Per-state prevalence, showing the fraction of time each state was marked as positive across subjects. (Bottom) Intensity distributions for confusion, hesitation, and readiness, averaged across subjects, with bars indicating the relative frequency of low, medium, and high intensities.

a broader spread, including notable fractions of medium- and high-intensity segments. Readiness, in contrast, was rarely annotated and was dominated by high-intensity marks. Together, these distributions highlight class imbalance across states and intensity levels, underscoring the challenge of reliably modeling nuanced cognitive processes from motion data when cognitive states are absent in most of the dataset.

### 4.2 Annotation Reliability

To assess the reliability of the text-based description and rating task (see Sec. 3.3), we measured agreement between each descriptor’s self-report and the two independent raters who judged whether the description reflected Confusion, Hesitation, or Readiness. Agreement was quantified using Cohen’s  $\kappa$ , computed per state and averaged across descriptors.

We observed substantial agreement for Confusion ( $\kappa = 0.69$ ) and Hesitation ( $\kappa = 0.62$ ), and almost perfect agreement for Readiness ( $\kappa = 0.95$ ). The overall mean across states was  $\kappa = 0.75$ . These results indicate that participants reached an agreement when interpreting and distinguishing between confusion, hesitation, and readiness when evaluating decision-making processes, supporting the reliability of our dataset annotations.

### 4.3 Experiment Design

We designed our experiments to systematically vary both the *feature representation* and the *output formulation*, under two distinct training schemas. This allows us to disentangle the effect of representation, label granularity, and subject overlap in the training/test split.

Table 1: Setting 1 - Pooled features, binary classification, 70/30 split. Input:  $[B, 105]$ , Output:  $[B, 8]$ . The highest value is highlighted in **bold**.

Model	Overall					Reading					Confusion					Hesitation					Readiness				
	Acc.	Prec.	Rec.	F1	IoU	Acc.	Prec.	Rec.	F1	IoU	Acc.	Prec.	Rec.	F1	IoU	Acc.	Prec.	Rec.	F1	IoU	Acc.	Prec.	Rec.	F1	IoU
Human	<b>0.793</b>	<b>0.458</b>	0.455	<b>0.431</b>	<b>0.344</b>	<b>0.850</b>	<b>0.804</b>	<b>0.903</b>	<b>0.839</b>	<b>0.728</b>	0.747	0.282	0.242	0.243	<b>0.174</b>	0.658	0.621	0.556	0.543	0.409	<b>0.916</b>	0.124	0.119	0.099	0.066
SVM	0.744	0.412	0.247	0.292	0.198	0.670	0.706	0.490	0.579	0.407	0.798	0.143	0.013	0.023	0.012	0.590	0.586	0.454	0.512	0.344	<b>0.916</b>	<b>0.214</b>	0.031	0.054	0.028
RF	0.779	0.435	0.307	0.344	0.250	0.719	0.742	0.600	0.663	0.496	<b>0.800</b>	0.303	0.042	0.074	0.038	0.682	<b>0.695</b>	0.588	0.637	0.467	<b>0.916</b>	0.000	0.000	0.000	0.000
LightGBM	0.778	0.462	0.349	0.385	0.278	0.714	0.742	0.582	0.652	0.484	0.791	<b>0.360</b>	0.131	0.192	0.106	<b>0.696</b>	0.682	0.672	<b>0.677</b>	<b>0.512</b>	0.911	0.062	0.010	0.018	0.009
LSTM	0.623	0.376	0.475	0.397	0.272	0.656	0.653	0.544	0.594	0.422	0.614	0.194	<b>0.329</b>	<b>0.244</b>	0.139	0.625	0.589	<b>0.688</b>	0.634	0.465	0.598	0.070	<b>0.340</b>	0.116	0.062
ResNet	0.684	0.398	<b>0.484</b>	0.426	0.299	0.680	0.656	0.646	0.651	0.483	0.654	0.205	0.287	0.239	0.136	0.660	0.628	0.693	0.659	0.491	0.741	0.105	0.309	<b>0.156</b>	<b>0.085</b>

Table 2: Setting 2 - Pooled features, binary classification, LOSO split. Input:  $[B, 105]$ , Output:  $[B, 8]$ . The highest value is highlighted in **bold**.

Model	Overall					Reading					Confusion					Hesitation					Readiness				
	Acc.	Prec.	Rec.	F1	IoU	Acc.	Prec.	Rec.	F1	IoU	Acc.	Prec.	Rec.	F1	IoU	Acc.	Prec.	Rec.	F1	IoU	Acc.	Prec.	Rec.	F1	IoU
Human	<b>0.793</b>	<b>0.458</b>	0.455	<b>0.431</b>	<b>0.344</b>	<b>0.850</b>	<b>0.804</b>	<b>0.903</b>	<b>0.839</b>	<b>0.728</b>	0.747	<b>0.282</b>	0.242	<b>0.243</b>	<b>0.174</b>	<b>0.658</b>	<b>0.621</b>	<b>0.556</b>	<b>0.543</b>	<b>0.409</b>	0.916	0.124	0.119	0.099	0.066
SVM	0.718	0.326	0.257	0.231	0.161	0.615	0.611	0.544	0.525	0.381	0.797	0.110	0.035	0.027	0.015	0.538	0.549	0.440	0.361	0.242	<b>0.919</b>	0.033	0.007	0.011	0.007
RF	0.739	0.325	0.250	0.251	0.177	0.650	0.685	0.510	0.547	0.401	<b>0.799</b>	0.024	0.041	0.027	0.016	0.589	0.591	0.449	0.428	0.292	<b>0.919</b>	0.000	0.000	0.000	0.000
LightGBM	0.740	0.373	0.264	0.270	0.190	0.649	0.688	0.492	0.540	0.391	0.798	0.202	0.046	0.056	0.031	0.597	0.539	0.512	0.477	0.333	0.915	0.062	0.004	0.007	0.004
LSTM	0.586	0.328	0.452	0.275	0.187	0.551	0.519	0.589	0.472	0.343	0.575	0.211	<b>0.448</b>	0.204	0.123	0.528	0.512	0.453	0.342	0.236	0.692	0.070	0.316	0.081	0.046
ResNet	0.603	0.323	<b>0.470</b>	0.307	0.211	0.586	0.548	0.623	0.515	0.382	0.581	0.172	0.420	0.206	0.123	0.544	0.443	0.485	0.383	0.268	0.699	<b>0.127</b>	<b>0.352</b>	<b>0.125</b>	<b>0.070</b>

**Feature representation.** We consider two approaches: (1) **Pooled features**, where motion signals within a temporal window are aggregated into a fixed-length vector using statistical summaries. This removes temporal ordering and yields a single prediction per window. (2) **Sequential features**, where the raw frame-wise sequence within a window is preserved, allowing models to capture temporal dependencies and produce frame-level predictions.

**Output formulation.** We evaluate both: (1) **Binary classification**, where each state is predicted as present or absent, collapsing intensity levels. (2) **Multi-class classification**, where full label levels are preserved ( $\{\text{none, low, medium, high}\}$  for Confusion, Hesitation, and Readiness; binary for Reading).

**Training schemas.** We employ two splitting strategies:

(1) **Leave-One-Subject-Out (LOSO)**, where the model is trained on all but one participant and tested on the held-out participant. This setting evaluates generalization to unseen subjects.

(2) **Within-Participant Split (70/30)**, where we first split each participant’s full time series at the 70% elapsed time: the first 70% forms a trial pool for training, the last 30% a trial pool for testing. We then generate sliding windows independently within each pool (window=2 s, stride=0.5 s) to construct train/test windows. No window spans the 70/30 boundary.

**Experimental settings.** Combining these factors yields the following configurations, each contributing a result table:

- `pooled_binary_37`: Pooled features, binary classification, 70/30 split.
- `pooled_binary_loso`: Pooled features, binary classification, LOSO split.
- `pooled_ordinal_37`: Pooled features, multi-class classification, 70/30 split.
- `seq_binary_37`: Sequential features, binary classification, 70/30 split.

This design isolates the impact of representation (pooled vs. sequential), label granularity (binary vs. ordinal), and subject overlap in training (LOSO vs. 70/30).

#### 4.4 Human and Model Performance under Within-Participant Split

Table 1 reports results under the 70/30 within-participant split (`pooled_binary_37`). In this setting, the model is trained on a portion of each participant’s data and tested on the remaining clips, allowing partial exposure to the same participants during training. For reference, we also include the human baseline (Sec. 3.6), where participants annotated masked clips from others without training.

We find that models reach performance comparable to human observers. The overall F1 of ResNet is 0.426, close to the human F1 of 0.431. And ResNet outperformed the human baseline in overall recall. Besides, Random Forest achieved the highest overall accuracy of 0.779 among models, comparable to that of human observers. In particular, models detect hesitation with accuracy close to human level, while confusion remains more difficult for both. Readiness shows the highest agreement, reflecting its clearer motion signature.

These results indicate that when the model can learn from part of each participant’s motion, it can approximate human-level recognition of cognitive states. This provides an upper-bound on achievable performance before testing cross-participant generalization in LOSO (Sec. 4.5).

#### 4.5 Generalization Across Participants: LOSO Evaluation

Table 1 summarizes results under the 70/30 within-participant split, while Table 2 shows results under the Leave-One-Subject-Out (LOSO) setting. In the within-participant case, the model is trained on a portion of each participant’s data and tested on the remaining clips, allowing partial exposure to the same individuals. In contrast, LOSO strictly holds out all data from one participant for testing, preventing the model from seeing that subject’s motion during training.

We observe a consistent performance drop when moving from the within-participant split to LOSO. For example, the overall F1-score of ResNet decreases from 0.426 to 0.307, and LightGBM drops from 0.365 to 0.270. Similar declines are seen across most states and metrics. This suggests that models benefit from participant-specific motion patterns under the 70/30 split, but struggle to generalize once such overlap is removed.

These findings emphasize the challenge of subject-independent modeling of cognitive states. While the within-participant setting provides an upper bound on achievable performance, LOSO more accurately reflects deployment in real-world scenarios where models must handle entirely unseen users. The observed gap highlights

Table 3: Setting 3 - Pooled features, multi-class classification, 70/30 split. Input:  $[B, 105]$ , Output:  $[B, 14]$ . The highest value is highlighted in **bold**.

Model	Overall				Reading				Confusion				Hesitation				Readiness								
	Acc.	Prec.	F1	IoU																					
Human	<b>0.756</b>	<b>0.517</b>	<b>0.546</b>	<b>0.514</b>	<b>0.450</b>	<b>0.850</b>	<b>0.804</b>	<b>0.903</b>	<b>0.839</b>	<b>0.728</b>	0.725	<b>0.422</b>	<b>0.423</b>	<b>0.405</b>	<b>0.350</b>	<b>0.538</b>	0.322	0.326	0.293	0.227	0.911	<b>0.521</b>	<b>0.532</b>	<b>0.521</b>	<b>0.497</b>
SVM	0.731	0.407	0.320	0.327	0.256	0.670	0.706	0.490	0.579	0.407	0.804	0.244	0.251	0.228	0.204	0.537	<b>0.446</b>	0.291	0.263	0.183	0.913	0.231	0.247	0.239	0.229
RF	0.743	0.402	0.359	0.368	0.290	0.719	0.742	0.600	0.663	0.496	<b>0.799</b>	0.265	0.255	0.240	0.209	<b>0.538</b>	0.369	0.332	0.329	0.224	<b>0.916</b>	0.230	0.248	0.239	0.229
LightGBM	0.733	0.431	0.356	0.369	0.285	0.691	0.709	0.562	0.627	0.456	0.792	0.388	0.263	0.256	0.216	0.535	0.369	<b>0.349</b>	<b>0.347</b>	<b>0.237</b>	0.912	0.258	0.250	0.244	0.231
LSTM	0.432	0.341	0.356	0.301	0.200	0.618	0.596	0.539	0.566	0.395	0.328	0.235	0.260	0.188	0.115	0.253	0.293	0.311	0.198	0.144	0.527	0.238	0.316	0.145	0.200
ResNet	0.444	0.351	0.393	0.317	0.211	0.628	0.604	0.565	0.584	0.412	0.337	0.245	0.293	0.196	0.120	0.266	0.284	0.300	0.239	0.143	0.545	0.272	0.412	0.239	0.169

Table 4: Setting 4 - Sequential features, binary classification, 70/30 split. Input:  $[B, T, 69]$ , Output:  $[B, T, 8]$ . The highest value is highlighted in **bold**.

Model	Overall				Reading				Confusion				Hesitation				Readiness								
	Acc.	Prec.	F1	IoU	Acc.	Prec.	F1	IoU	Acc.	Prec.	F1	IoU	Acc.	Prec.	F1	IoU	Acc.	Prec.	F1	IoU					
Human	<b>0.820</b>	<b>0.406</b>	0.412	<b>0.382</b>	<b>0.288</b>	<b>0.810</b>	<b>0.698</b>	<b>0.803</b>	<b>0.726</b>	<b>0.578</b>	<b>0.820</b>	<b>0.264</b>	0.227	0.221	<b>0.155</b>	<b>0.714</b>	<b>0.564</b>	0.524	0.502	0.369	<b>0.934</b>	<b>0.096</b>	0.095	0.080	0.051
LSTM	0.672	0.294	0.422	0.335	0.216	0.668	0.465	0.537	0.498	0.332	0.652	0.146	0.260	0.187	0.103	0.623	0.489	0.583	0.532	0.362	0.746	0.076	0.308	0.122	0.065
ResNet	0.685	0.323	0.475	0.369	0.243	0.703	0.514	0.583	0.547	0.376	0.674	0.177	<b>0.308</b>	<b>0.225</b>	0.127	0.652	0.521	<b>0.638</b>	<b>0.574</b>	<b>0.402</b>	0.712	0.078	<b>0.372</b>	<b>0.129</b>	<b>0.069</b>

the importance of designing approaches that are robust to inter-individual variability in motion patterns.

#### 4.6 Multi-Class Classification of Cognitive State Intensity

Table 3 presents results under the multi-class setting, where models are trained to differentiate between four intensity levels (no/low/medium/high) for each state. Compared to the binary classification results in Table 1, this task is more challenging because it requires finer discrimination between subtle variations in motion patterns that reflect different levels of cognitive states.

Human performance shows only a modest drop when moving from binary to multi-class classification, with overall accuracy decreasing from 0.793 to 0.756. This suggests that human observers can distinguish intensity levels to some degree, particularly for readiness, where performance remains strong. By contrast, models exhibit a larger performance decline in the multi-class setting. For example, ResNet’s overall F1 decreases from 0.426 in the binary task to 0.317 in the multi-class task. Similar declines are observed across LSTM and LightGBM, indicating that these models struggle to separate subtle gradations of cognitive states.

Notably, classical machine learning models such as Support Vector Machines (SVM), Random Forest (RF) and LightGBM, achieve performance that is competitive with or better than more complex deep temporal models in this setting. This outcome highlights that lightweight, classical methods may retain advantages when the classification task depends on small differences between intensity levels, whereas deep models may overfit without sufficient signal.

Together, these findings suggest that while both humans and models can identify the presence of cognitive states, humans remain more reliable at judging intensity. Improving model performance on this finer-grained task may require richer representations, larger datasets, or multimodal signals that capture subtle motion cues more effectively.

#### 4.7 Sequential Features and Frame-Level Prediction

Table 4 presents results under the sequential binary classification setting, where models are trained to predict states frame by frame rather than pooling features across a window (Table 1). This design allows models to directly exploit temporal dynamics, but increases the difficulty of the task due to noisy frame-level variability.

Only deep temporal models were tested here (LSTM, ResNet), since classical models cannot explicitly capture sequential dependencies. Compared to pooled features, frame-level predictions yield modest changes in performance. For example, ResNet’s overall F1 decreases from 0.426 in the pooled setting to 0.369 in the sequential setting, while LSTM shows a similar drop (0.397 to

0.335). These results suggest that temporal models can leverage fine-grained motion cues but are also more sensitive to label sparsity and noise.

Humans remain more robust across the two conditions. The overall human F1 under sequential evaluation is 0.382, only slightly lower than the pooled binary setting (0.431). However, a closer breakdown reveals that humans achieve higher accuracy and precision, but lower recall and F1 on confusion, hesitation, and readiness compared to LSTM and ResNet. This pattern reflects class imbalance: human annotators tend to favor the majority “no-state” class, producing high accuracy but missing many true positives. In contrast, deep temporal models better detect periods when participants experience specific cognitive states, highlighting their ability to capture nuanced frame-level differences in motion.

## 5 DISCUSSION

### 5.1 Main Findings

Our results provide the first systematic evidence that standard VR motion data encodes signals of nuanced cognitive states. When models were trained with partial exposure to individual participants (70/30 split), they approached the human baseline, particularly for hesitation and readiness, which appear to have stronger motion signatures. However, performance dropped sharply under Leave-One-Subject-Out evaluation, underscoring the difficulty of subject-independent inference.

Multi-class classification further revealed that humans remain more reliable in distinguishing intensity levels, while models struggle to capture subtle gradations. Sequential frame-level modeling allowed temporal models to detect brief periods of hesitation, but also amplified sensitivity to label sparsity and noise. Together, these results show that motion alone is a viable and sensitive signal of cognitive states.

### 5.2 Implications

These findings establish that motion telemetry is a viable signal for inferring nuanced cognitive states in VR, with potential applications in adaptive systems:

- **Adaptive training:** Systems could provide timely guidance when hesitation or confusion is detected.
- **Social VR and collaboration:** Avatars enriched with inferred states (e.g., hesitation) could signal uncertainty and facilitate smoother communication.
- **Accessibility:** Interfaces could modulate complexity in real time to support users experiencing confusion or cognitive

overload, or move quickly to the next step if readiness is detected.

At the same time, the ability to infer internal states from motion raises critical privacy issues. Motion signals have been shown to be highly identifying at the individual level; when combined with cognitive state inference, they could expose highly sensitive information. Any practical system must therefore include safeguards such as transparency, user consent, and strict data governance.

### 5.3 Limitations and Future Work

This study has several limitations. The dataset was collected from 24 participants in a controlled lab environment, which constrains diversity and ecological validity. Annotations relied on subjective self-reports, which may not perfectly capture underlying states. The analysis was aimed at examining the potential of head and hand motion, and therefore excluded other potentially informative modalities such as eye tracking, facial expressions, or physiological signals.

Future work should expand to larger and more diverse populations, test models in real-world VR scenarios, and explore multimodal integration. Combining motion data with complementary signals, or with contextual language cues, may improve sensitivity to subtle intensity levels. In addition, advancing subject-independent training strategies and real-time deployment will be essential for adaptive VR applications.

## 6 CONCLUSION

We presented a novel dataset and modeling framework for inferring confusion, hesitation, and readiness from solely VR head and hand motion. Our experiments show that models trained on motion alone can approach human baselines under within-participant evaluation, confirming that these subtle states leave detectable traces in standard VR telemetry.

However, performance declines substantially when generalizing across unseen users and when distinguishing between intensity levels. These results highlight both the promise and the fragility of motion-based cognitive state inference.

In summary, this work establishes a foundation for adaptive VR systems that respond to users' internal states in real time. At the same time, it underscores the need for privacy safeguards and fairness considerations, ensuring that future systems leverage this capability responsibly.

## REFERENCES

- [1] E. Aksan, M. Kaufmann, P. Cao, and O. Hilliges. A spatio-temporal transformer for 3d human motion prediction. In *2021 International Conference on 3D Vision (3DV)*, pp. 565–574. IEEE, 2021. 3
- [2] Y. S. Aurelio, G. M. De Almeida, C. L. de Castro, and A. P. Braga. Learning from imbalanced data sets with weighted cross-entropy function. *Neural processing letters*, 50(2):1937–1949, 2019. 5
- [3] N. Avital, E. Nahum, G. C. Levi, and D. Malka. Cognitive state classification using convolutional neural networks on gamma-band eeg signals. *Applied Sciences*, 14(18):8380, 2024. 2
- [4] X. Du, J. Wu, X. Tang, X. Lv, L. Jia, and C. Xue. Predicting user attention states from multimodal eye–hand data in vr selection tasks. *Electronics*, 14(10):2052, 2025. 2
- [5] A. Dutta, A. Gupta, and A. Zissermann. Vgg image annotator (via), 2016. 4
- [6] M. Gahalawat, R. Fernandez Rojas, T. Guha, R. Subramanian, and R. Goecke. Explainable depression detection via head motion patterns. In *Proceedings of the 25th International Conference on Multimodal Interaction*, pp. 261–270, 2023. 1
- [7] G. W. Hart. Nonintrusive appliance load monitoring. *Proceedings of the IEEE*, 80(12):1870–1891, 1992. 2
- [8] S. Hochreiter and J. Schmidhuber. Long short-term memory. *Neural computation*, 9(8):1735–1780, 1997. 2
- [9] C.-J. Hsu, K.-S. Huang, C.-B. Yang, and Y.-P. Guo. Flexible dynamic time warping for time series classification. *Procedia Computer Science*, 51:2838–2842, 2015. 2
- [10] S. Idrees, J. Choi, and S. Sohn. Advmt: Adversarial motion transformer for long-term human motion prediction. *arXiv preprint arXiv:2401.05018*, 2024. 3
- [11] C. M. A. Ilyas, R. Nunes, K. Nasrollahi, M. Rehm, and T. B. Moeslund. Deep emotion recognition through upper body movements and facial expression. In *VISIGRAPP (5: VISAPP)*, pp. 669–679, 2021. 2
- [12] H. Ismail Fawaz, G. Forestier, J. Weber, L. Idoumghar, and P.-A. Muller. Deep learning for time series classification: a review. *Data mining and knowledge discovery*, 33(4):917–963, 2019. 3
- [13] K. Kedia, A. Bhardwaj, P. Dan, and S. Choudhury. Interact: Transformer models for human intent prediction conditioned on robot actions. In *2024 IEEE International Conference on Robotics and Automation (ICRA)*, pp. 621–628. IEEE, 2024. 3
- [14] D. P. Kingma. Adam: A method for stochastic optimization. *arXiv preprint arXiv:1412.6980*, 2014. 5
- [15] A. F. Laudanski, A. Küderle, F. Kluge, B. M. Eskofier, and S. M. Acker. High-knee-flexion posture recognition using multi-dimensional dynamic time warping on inertial sensor data. *Sensors*, 25(4):1083, 2025. 2
- [16] J. Li, D. Chen, T. Cai, P. Chen, Y. Hong, Z. Chen, Y. Shen, and C. Gan. Flexattention for efficient high-resolution vision-language models. In *European Conference on Computer Vision*, pp. 286–302. Springer, 2024. 3
- [17] Z. Lin, M. Feng, C. N. d. Santos, M. Yu, B. Xiang, B. Zhou, and Y. Bengio. A structured self-attentive sentence embedding. *arXiv preprint arXiv:1703.03130*, 2017. 3
- [18] J. L. Lobo, J. D. Ser, F. De Simone, R. Presta, S. Collina, and Z. Moravek. Cognitive workload classification using eye-tracking and eeg data. In *Proceedings of the international conference on human-computer interaction in aerospace*, pp. 1–8, 2016. 2
- [19] N.-D. Mai, B.-G. Lee, and W.-Y. Chung. Affective computing on machine learning-based emotion recognition using a self-made eeg device. *Sensors*, 21(15):5135, 2021. 2
- [20] E. V. Mascaró, S. Ma, H. Ahn, and D. Lee. Robust human motion forecasting using transformer-based model. In *2022 IEEE/RSJ International Conference on Intelligent Robots and Systems (IROS)*, pp. 10674–10680. IEEE, 2022. 3
- [21] M. R. Miller, F. Herrera, H. Jun, J. A. Landay, and J. N. Bailenson. Personal identifiability of user tracking data during observation of 360-degree vr video. *Scientific Reports*, 10(1):17404, 2020. 2
- [22] V. Nair, W. Guo, J. Mattern, R. Wang, J. F. O'Brien, L. Rosenberg, and D. Song. Unique identification of 50,000+ virtual reality users from head & hand motion data. In *32nd USENIX Security Symposium (USENIX Security 23)*, pp. 895–910, 2023. 2, 4
- [23] R. Niels. Dynamic time warping. *Artificial Intelligence*, 2004. 2
- [24] A. Oğuz and Ö. F. Ertuğrul. Emotion recognition by skeleton-based spatial and temporal analysis. *Expert Systems with Applications*, 238:121981, 2024. 2
- [25] J. W. Payne, J. R. Bettman, and E. J. Johnson. *The adaptive decision maker*. Cambridge university press, 1993. 2
- [26] P. Pirolli and S. Card. Information foraging. *Psychological review*, 106(4):643, 1999. 2
- [27] S. Sandeep, C. R. Shelton, A. Pahor, S. M. Jaeggi, and A. R. Seitz. Application of machine learning models for tracking participant skills in cognitive training. *Frontiers in Psychology*, 11:1532, 2020. 2
- [28] S. Seo, S. Yoo, H. Lee, Y. Jang, J. H. Park, and J.-N. Kim. A sentence-level visualization of attention in large language models. In *Proceedings of the 2025 Conference of the Nations of the Americas Chapter of the Association for Computational Linguistics: Human Language Technologies (System Demonstrations)*, pp. 313–320, 2025. 3
- [29] F. Serpush, M. B. Menhaj, B. Masoumi, and B. Karasfi. Wearable sensor-based human activity recognition in the smart healthcare system. *Computational intelligence and neuroscience*, 2022(1):1391906, 2022. 2
- [30] H. A. Simon. A behavioral model of rational choice. *The quarterly journal of economics*, pp. 99–118, 1955. 2
- [31] A. Singh, B. T. Le, T. L. Nguyen, D. Whelan, M. O'Reilly,

- B. Caulfield, and G. Ifrim. Interpretable classification of human exercise videos through pose estimation and multivariate time series analysis. In *International Workshop on Health Intelligence*, pp. 181–199. Springer, 2021. 2
- [32] Y. Sun, M. Cabezas, J. Lee, C. Wang, W. Zhang, F. Calamante, and J. Lv. Predicting human brain states with transformer. In *International Conference on Medical Image Computing and Computer-Assisted Intervention*, pp. 136–146. Springer, 2024. 3
- [33] Y. Suzuki, F. Wild, and E. Scanlon. Measuring cognitive load in augmented reality with physiological methods: A systematic review. *Journal of Computer Assisted Learning*, 40(2):375–393, 2024. 2
- [34] A. Vaswani, N. Shazeer, N. Parmar, J. Uszkoreit, L. Jones, A. N. Gomez, Ł. Kaiser, and I. Polosukhin. Attention is all you need. *Advances in neural information processing systems*, 30, 2017. 3
- [35] Y. Wang, J. Wang, X. Liu, and T. Zhu. Detecting depression through gait data: examining the contribution of gait features in recognizing depression. *Frontiers in psychiatry*, 12:661213, 2021. 1
- [36] K. Xu, J. Ba, R. Kiros, K. Cho, A. Courville, R. Salakhudinov, R. Zemel, and Y. Bengio. Show, attend and tell: Neural image caption generation with visual attention. In *International conference on machine learning*, pp. 2048–2057. PMLR, 2015. 3
- [37] Z. Yan and W. Fan. Biomechanical data-driven prediction and analysis based on transformer model. *Molecular & Cellular Biomechanics*, 22(2):1235–1235, 2025. 3
- [38] L. Zeng. Predicting user grasp intentions in virtual reality. *arXiv preprint arXiv:2508.16582*, 2025. 2
- [39] J. Zhang, M. Lau, and Z. Zhu. Hybrid cnn-gru model for exercise classification using imu time-series data. *Journal of Machine Intelligence and Data Science (JMIDS)*, 5(1):54–64, 2024. 3
- [40] Y. Zhang, Y. Zhang, Z. Zhang, J. Bao, and Y. Song. Human activity recognition based on time series analysis using u-net. *arXiv preprint arXiv:1809.08113*, 2018. 3